ORIGINAL PAPER

DOI: http://dx.doi.org/10.15403/jgld-4219

Computed Tomography for the Diagnosis of Intraperitoneal Infected Fluid Collections after Surgery for Gastric Cancer. Role of Texture Analysis

Vlad-Radu Puia[1,2], Aida Puia[1], Alin-Cornel Fetti[1,2], Paul-Andrei Ștefan[1,3], Dan Vălean[2], Andrei Herdean[1], Ioana Rusu[4], Tudor Vasile[5], Andrei Lebovici[1,5], Nadim Al-Hajjar[1,2]

1) Iuliu Haţieganu University of Medicine and Pharmacy, Cluj-Napoca;
2) Surgery Department, Octavian Fodor Regional Institute of Gastroenterology and Hepatology, Cluj-Napoca;
3) Radiology and Imaging Department, County Emergency Hospital, Cluj-Napoca;
4) Pathology Department, Octavian Fodor Regional Institute of Gastroenterology and Hepatology, Cluj-Napoca;
5) Radiology and Imaging Department, Octavian Fodor Regional Institute of Gastroenterology and Hepatology, Cluj-Napoca, Romania

Address for correspondence:
Aida Puia
Iuliu Haţieganu University of Medicine and Pharmacy, Cluj-Napoca, Romania
draidapuia@gmail.com

Received: 19.01.2022
Accepted: 02.03.2022

ABSTRACT

Background & Aims: Several computed tomographic (CT) imaging features have been proposed to describe the infection of postoperative abdominal fluid collections; however, these features are vague, and there is a significant overlap between infected and non-infected collections. We assessed the role of textural parameters as additional diagnostic tools for distinguishing between infected and non-infected peritoneal collections in patients operated for gastric cancer.

Methods: From 527 patients operated for gastric cancer, we retrospectively selected 82 cases with intraperitoneal collections who underwent CT exams. The fluid component was analyzed through a novel method (texture analysis); different patterns of pixel intensity and distribution were extracted and processed through a dedicated software (MaZda). A univariate analysis comparing the parameters of texture analysis between the two groups was performed. Afterwards, a multivariate analysis was performed for the univariate statistically significant parameters.

Results: The study included 82 patients with bacteriologically verified infected (n=40) and noninfected (n=42) intraperitoneal effusions. The univariate analysis evidenced statistically significant differences between all the parameters involved. The multivariate analysis highlighted 10 parameters as being statistically significant, adjusted to Bonferroni correction.

Conclusions: Our evidence supports the fact that textural analysis can be used as a complementary diagnostic tool for the detection of infected fluid collections after gastric cancer surgery. Further studies are required to validate the accuracy of this method.

Key words: peritoneal collections – computed tomography – texture-based analysis – gastric cancer – surgery.

Abbreviations: CT: computed tomography; IPE: intra-peritoneal effusions; ROI: region of interest; TA: texture analysis.

INTRODUCTION

Abdominal fluid collections are common after surgery, with imaging studies reporting an incidence of up to 64% [1]. Regardless of their content, all these fluid collections have the potential to become infected, resulting in the formation of an abscess. Radiologists and practitioners are urged to evaluate the underlying etiology of infection, such as anastomotic leakage, when there is a suspicion of abscess formation following surgery [2].

To avoid increased morbidity and mortality, it is critical to distinguish between infected and noninfected abdominal fluid collections after surgery. Abscesses are frequently treated surgically or percutaneously, although in the case of noninfected abdominal collections, invasive treatment should be avoided [3].

The clinical importance of a correct diagnosis in the postoperative period is demonstrated by the fact that mortality from infected abdominal fluid collections ranges from 30% in treated cases to 80-100% in patients with undrained and non-operated abscesses [4, 5].

The most common imaging modality to identify and characterize the postoperative abdominal fluid accumulation is computed tomography (CT). In order to distinguish infected from noninfected collections, fluid attenuation measures, encapsulation, stranding of the surrounding fat, and the presence of gas within the collection were proposed. However, these CT imaging parameters are nonspecific, because infected

and noninfected fluid collections overlap significantly with an accuracy ranging between 56-82% [5-8].

Intra-peritoneal effusions (IPE) as little as 50 mL can be detected using a CT scan. The pathological examination of the fluid reveals that IPE has unique biochemical, cytological, and physical characteristics. These features must be translated in CT scans to provide extra diagnostic information, but they are challenging to quantify during standard medical image interpretation [9-11]. The pixels in a computer image produce patterns of forms and colors which are referred to as textures [12]. Texture analysis (TA) is a technique for providing an objective description of image contents by quantifying the distribution patterns and intensity of pixels. It is based on the extraction and processing of image-specific information [13].

In the present study we used TA to quantify the image features of IPE on CT images. The aim was to determine if texture parameters could provide additional diagnostic information to be used as a non-invasive criterion for distinguishing between infected and non-infected IPE in patients operated for gastric cancer.

METHODS

Study Population

This is a retrospective study undertaken for the period January 2016 to December 2020, in which 527 patients were operated for gastric cancer. We selected patients diagnosed with gastric malignant tumors (histological confirmed), radically operated (total or partial gastrectomy, multiorgan resections) and presented IPE after surgery, identified on CT scan. The inclusion criteria were: 1) collections with a diameter of at least 30 mm; 2) absence of imaging artifacts 3) peritoneal fluid harvested in the next 7 days after performing the CT.

Based on bacteriological results of the aspirated fluid we grouped our patients in an infected IPE and a non-infected IPE group. The infected collections arose in patients who developed postoperative fistula and were objectified by CT and/or during surgery. Ultrasound-guided puncture or surgical reinvention was performed in these cases.

Computed Tomography Protocol and Texture Analysis

All CT scans were performed on the same unit, Siemens Somatom Sensation, 16 slices (Siemens medical solutions, Forchheim, Germany). The CT scan covered the region from the dome of the liver to the ischial tuberosity attachment. The parameters of the CT scan were 120 kV, 200 mAs and 3 mm slice thickness.

Radiomics represents the extraction of quantitative information from clinical imaging [14]. A radiomic metric called TA has been reported to assess tissue heterogeneity from medical images in studies investigating the diagnosis, prognosis, and treatment response of different pathologies [15]. Through extraction and processing of specific imaging parameters, this technique provides a quantitative description of image contents that cannot be assessed through the usual interpretation of medical images.

Texture analysis has been incorporated in various stages of the radiomics workflow. Images might be segmented into contiguous regions based on the texture properties of each region during the preprocessing stage, and texture features could provide clues for classifying patterns or recognizing objects during the feature extraction and classification phases [16].

The radiomics approach consisted of four steps: image segmentation using regions of interest, feature extraction, feature selection, and prediction.

Image Pre-Processing and Segmentation

Each examination was reviewed on a dedicated workstation (General Electric, Advantage workstation, 4.7 edition) by one radiologist. On the non-enhanced phase of each examination a single slice was chosen considered the most representative for the fluid content. All examinations were anonymized, and the selected slices were retrieved in DICOM format (Digital Imaging and Communications in Medicine). A second researcher imported each image into a TA software, MaZda version 5.

Image Segmentation

For the segmentation step, the same researcher incorporated the ascitic fluid in a two-dimensional (2D) region of interest (ROI). A semi-automatic level-set technique was used for the definition and positioning of each ROI. The researcher placed a seed in the approximate center of the fluid collection and the software automatically delineated the collection based on gradient coordinates (Fig. 1).

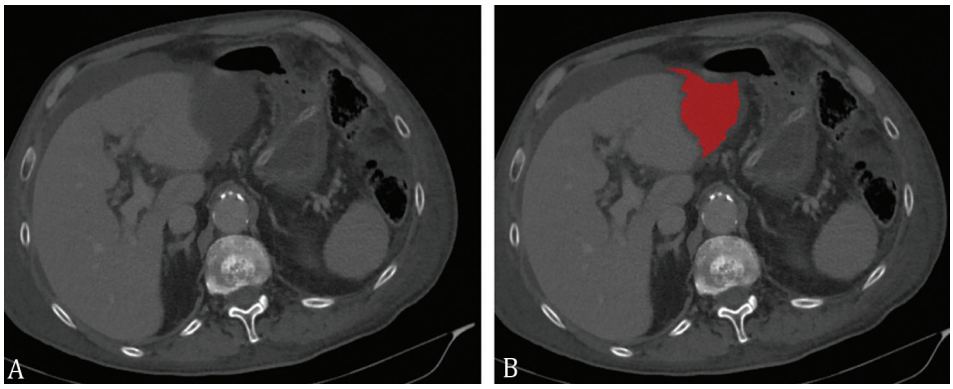

Fig. 1. (A) Axial CT non-enhanced phase image of a 61-year-old patient with non-infected fluid collection following surgery. (B) The slice with the region of interest (red area) used for texture analysis.

Feature Extraction

The feature extraction was automatically performed by the built-in tools of the MaZda software. The analysis of every ROI resulted in 275 texture parameters which originated from the grey-level histogram, the wavelet transformation, the co-occurrence matrix, the run-length matrix, the absolute gradient, and the autoregressive model.

Abbreviations of feature characteristics produced by the extraction algorithm appear in the feature name generated by MaZda software. The first imaging processing procedure is indicated by the leftmost symbol. The color channel is indicated by the first letter ("C" implies that a black and grey image was computed, "R" identities the red color channel). Image normalization is represented by the second symbol (N) after which follows the encoding for the method used, in this case, "S" represents image normalization using the limitation of dynamics to $\mu \pm 3\sigma$. The number after that indicates that the feature was quantized to use those numerous bits per pixel. The direction is coded using letters: H (horizontal), V (vertical), Z (45°), and N (135°). The extraction algorithm is identified by the next group of letters (e.g. Wav, haar wavelet transformation). The last group of letters is usually the feature name (LngREmph, long-run emphasis; ShrtREmp, short-run emphasis; En, energy)

The major parameter classes are displayed in the Table I.

Feature Selection

The MaZda program allows the selection of the most discriminative features through several reduction techniques. One such technique is represented by the Fisher method. The Fisher coefficient (F) defines the ratio of between-class variances to within-class variances. This method provides a set of ten features that have a high discriminatory ability [20]. Alongside the Fisher method, another selection technique based on the probability of classification error and average correlation coefficients (POE + ACC) was utilized [21]. By applying these selection methods, two sets, each containing ten features, were selected.

Statistical Analysis

The obtained data were collected using the Microsft Excel 2019 software. Absolute values recorded by the two types of fluids for each parameter were compared using a univariate analysis test (Mann–Whitney U), which is used to compare the median values between two independent variables, considering the p value smaller than 0.05 as statistically significant. Secondly, a multivariate analysis was conducted to investigate which of the parameters that showed statistically significant results at the univariate analysis were also independent predictors for infected collections, for the parameters showing p values below 0.0016 (using the Bonferroni correction) Statistical analysis was performed using a commercially available dedicated software, IBM Spss v26.0 (Armonk, NY, USA)

RESULTS

Of the 527 patients recorded in our department during the study period, 82 were retrospectively included in our study (36 male, mean age 68 years, age range 34-87 years). Subjects were divided according to the final bacteriology results of their sampled fluid into infected (n=40, 18 male) and noninfected IPEs (n=42, 18 male). The mean time between the CT examination and the fluid sampling was 4.7 days (range: 2-7 days). The infected collections were treated as follows: 7 patients required surgery per primam; 33 patients were initially treated conservatively by ultrasound-guided puncture and/or endoscopy (gastrointestinal stents, vacuum therapy with endo-sponge); 11 patient needed subsequent surgery after conservative management.

The features selected by the three reduction methods along with the univariate analysis results are displayed in Table II. Statistically significant differences were noted between the two groups for all 30 variables.

Table I. Texture analysis parameters

Textrure class	Texture parameters	Calculation	Variations	Total number of parameters
Run Length Matrix	RLNonUni, GLevNonU, LngREmph, ShrtREmp, Fraction	6 bits/pixel	4 directions	20
Absolute gradient	GrMean, GrVariance, GrSkewness, GrKurtosis, GrNonZeros, percentage of pixels with nonzero gradient	4 bits/pixel	-	5
Histogram	Mean, Variance, Skewness, Kurtosis, Perc.01 - 99%	-	-	5
Wavelet transformation	WavEn	5 scales	4 frequency bands	20
Co-occurrence Matrix	AngScMom, Contrast, Correlat, SumOfSqs, InvDfMom, SumAverg, SumVarnc, SumEntrp, Entropy, DifVarnc, DifEntrp	6 bits/pixel; 5 between-pixels distances	4 directions	220
Auto-regressive Model	Teta 1-4, Sigma	-	-	5

Mean: histogram's mean; variance: histogram's variance; skewness: histogram's skewness; Kurtosis: histogram's kurtosis; perc.01-99%: 1-99% percentile; GrMean: absolute gradient mean; GrVariance: absolute gradient variance; GrSkewness: absolute gradient skewness; GrKurtosis: absolute gradient kurtosis; GrNonZeros; RLNonUni: run-length nonuniformity; GLevNonU: grey level nonuniformity; LngREmph: long-run emphasis; ShrtREmp: short-run emphasis; fractionL the fraction of image in runs; AngScMom: angular second moment; correlat: correlation; SumOfSqs: the sum of squares; InvDfMom: inverse difference moment; SumAverg: sum average; SumVarnc: sum variance; SumEntrp: sum entropy; DifVarnc: difference variance; DifEntrp: difference entropy; Teta 1-4: parameters $\theta 1$ - $\theta 4$; Sigma: parameter σ; WavEn: wavelet energy.

Table II. The parameters selected by the reduction methods and the univariate analysis (Mann–Whitney U test) results

Parameter	Infected IPE group		Not infected IPE group		p
	Median	IQR	Median	IQR	
RVD6LngREmph	14.55	97.46	1.88	0.60	0.001
CH1D6Contrast	0.31	3.14	3.73	3.26	0.001
WavEnLH_s-2	0.69	16.45	12.48	29.00	0.001
RHD6RLNonUni	127.53	1032.78	733.00	1305.77	0.004
RHD6LngREmph	21.05	129.40	1.98	0.71	0.001
WavEnHL_s-2	0.50	9.39	12.38	27.85	0.000
CH2D6SumVarnc	0.61	12.65	9.30	9.54	0.002
RVD6RLNonUni	156.42	1052.17	747.40	1413.28	0.005
RND6LngREmph	11.75	56.03	1.66	0.48	0.001
WavEnHH_s-3	0.53	6.41	4.61	15.60	0.000
CH1D6DifVarnc	0.21	1.27	1.43	1.16	0.001
CZ1D6SumVarnc	0.62	14.50	10.16	10.56	0.002
CH1D6Contrast	0.31	3.14	3.73	3.26	0.001
CH1D6SumVarnc	0.74	17.08	12.99	11.54	0.002
CH1D6SumOfSqs	0.30	5.18	4.27	3.53	0.002
CV1D6SumVarnc	0.71	16.84	12.16	11.34	0.003
CH4D6DifVarnc	0.25	3.76	3.09	2.51	0.002
CN1D6SumVarnc	0.66	13.87	10.83	10.22	0.002
CN2D6SumVarnc	0.62	10.80	8.77	8.01	0.001
CV2D6SumVarnc	0.59	12.01	8.70	8.91	0.002
RND6Fraction	0.42	0.64	0.84	0.09	0.001
RZD6Fraction	0.44	0.65	0.84	0.06	0.000
RVD6Fraction	0.38	0.63	0.80	0.10	0.001
CZ2D6InvDfMom	0.79	0.55	0.36	0.09	0.001
RHD6Fraction	0.32	0.66	0.78	0.10	0.001
CN4D6InvDfMom	0.78	0.56	0.34	0.12	0.001
CV4D6InvDfMom	0.79	0.57	0.34	0.11	0.001
Perc01	964.50	934.00	82.00	22.75	0.000
Perc10	1002.50	930.75	91.00	12.75	0.000
CV3D6InvDfMom	0.79	0.56	0.35	0.09	0.001

For abbreviations see Table I.

All of the variables analyzed independently were taken into consideration for the multivariate analysis. Of the 30 variables, 10 were considered to be statistically significant, after the Bonferroni correction adjustment, as seen in Table III.

DISCUSSION

Even though the incidence and fatality rates of gastric cancer have significantly declined over time, it is still the second most common cancer worldwide [17].

One of the most significant complications of upper digestive tract surgery is infected intra-abdominal collections induced by a postoperative digestive fistula. In recent large-scale studies, the rate of post-operative digestive fistulas in gastric cancer surgery ranged from 0-26% to an average of 5-8% [18-20].

Sepsis is an increasing problem worldwide, with a 60% fatality rate [21, 22]. It primarily affects the elderly, immunologically compromised and severely ill patients. As a result, the diagnosis of sepsis must be made early, rapidly and precisely, necessitating immediate treatment.

In order to achieve a minimum level of bias, the study focused on a specific etiology regarding the infected/non-infected IPE. Our institution is focused on the oncological pathology of the digestive tract. In addition, there is a difference regarding the bacterial colonization in the upper gastrointestinal tract infections versus the lower gastrointestinal tract infections. Moreover, oncological patients tend to have a worse immune response towards infections than benign patients. The statements above support our decision to start our investigations with IPEs after upper gastrointestinal oncological surgery, mainly gastric cancer firsthand. This study can be considered a pathway towards expanding investigations of IPE collections in various gastrointestinal pathologies.

Table III. Multivariate analysis results

Source	Type III Sum of Squares	Mean Square	F	Sig.
RND6Fraction	1.593	1.593	29.873	0.000001624
RZD6Fraction	1.554	1.554	28.798	0.000002291
RVD6Fraction	1.517	1.517	28.033	0.000002936
CZ2D6InvDfMom	1.264	1.264	27.865	0.000003100
RHD6Fraction	1.523	1.523	27.716	0.000003256
CN4D6InvDfMom	1.251	1.251	27.620	0.000003359
CV4D6InvDfMom	1.263	1.263	27.513	0.000003479
Perc01	3140513.608	3140513.608	27.371	0.000003646
Perc10	3166532.216	3166532.216	27.135	0.000003940
CV3D6InvDfMom	1.239	1.239	27.093	0.000003995
RVD6LngREmph	394660.098	394660.098	2.827	0.099210372
CH1D6Contrast	41.352	41.352	3.204	0.079774575
WavEnLH_s-2	2647.604	2647.604	7.156	0.010185309
RHD6RLNonUni	6445031.937	6445031.937	4.651	0.036077709
RHD6LngREmph	154133.353	154133.353	8.180	0.006253162
WavEnHL_s-2	1231.429	1231.429	1.565	0.216989334
CH2D6SumVarnc	1172.417	1172.417	5.076	0.028867755
RVD6RLNonUni	6550035.622	6550035.622	4.555	0.037956424
RND6LngREmph	63133.986	63133.986	6.116	0.016986708
WavEnHH_s-3	2001.211	2001.211	7.121	0.010362803
CH1D6DifVarnc	7.222	7.222	4.049	0.049820731
CZ1D6SumVarnc	1033.905	1033.905	5.016	0.029780539
CH1D6Contrast	41.352	41.352	3.204	0.079774575
CH1D6SumVarnc	1796.816	1796.816	5.503	0.023162824
CH1D6SumOfSqs	148.959	148.959	5.625	0.021769200
CV1D6SumVarnc	1259.782	1259.782	5.386	0.024596931
CH4D6DifVarnc	46.266	46.266	5.407	0.024333945
CN1D6SumVarnc	1144.652	1144.652	5.743	0.020502502
CN2D6SumVarnc	691.498	691.498	5.552	0.022588687
CV2D6SumVarnc	672.456	672.456	5.316	0.025501324

For abbreviations see Table I.

Several CT imaging features have been proposed to detect infection of postoperative abdominal fluid collections, but the features are generic, and infected and non-infected collections show significant overlap [5]. Debris in an infected fluid collection generate enhanced CT attenuation, according to the fundamental idea behind measuring fluid collection attenuation. The relevance of attenuation measurements has been debated in previous research. Earlier studies discovered near-water attenuation of infected samples [23, 24], while a more recent investigation discovered attenuation levels more than 20 HU when infection was present [25].

Computer-aided diagnosis has become one of the most prominent topics in radiology. In recent years it has developed from a simple research problem to near implementation in clinical practice [26]. Texture analysis is a key feature of computer-aided diagnosis, and when combined with automated decision-making, it promises to revolutionize the way radiologists analyze images [27].

Our results show that four variations of the fraction parameter were independent predictors for infected collections.

The fraction of image in runs is a measure of the percentage of image pixels that are part of any of the runs considered for the matrix computing, and does not carry important diagnostic information [28].

Inverse difference moment is usually called homogeneity that measures the local homogeneity of an image. The inverse difference moment feature obtains the measures of the closeness of the distribution of the GLCM elements to the GLCM diagonal [29].

On all variations, we obtained higher values of this parameter for the infected group, most likely because the infected fluid had a more various cytology than the uninfected one.

The percentile number (n) is the point at which n% of the pixel values that form the histogram are found to the left. In other words, a percentile gives the highest gray-level value under which a given percentage of the pixels in the image are contained [30].

This signifies that 1% and 10% of the pixels within images were distributed under lower values for the non-infected IPE group. In other words, the infected group showed higher CT

densities, which probably correlates with the fluid density of these collections.

There are insufficient data in the current literature regarding textural analysis applied in infected collections post upper gastrointestinal surgery. Recent studies have shown differences regarding textural analysis in various fluid collections, focusing on differences between benign and malignant ascites; the studies also included, in a limited manner, an analysis to differentiate between infected and non-infected collections [11, 31].

CONCLUSIONS

With the help of TA we examined the tissue heterogeneity from the medical images in order to determine dif¬ferentiation criteria between infected and non-infected collection after gastric cancer surgery. In our study we obtained statistically significant results for the differentiation criteria. Our evidence supports the fact that textural analysis can be used as a complementary diagnostic tool for the detection of infected fluid collections after gastric cancer surgery. The emphasis can be placed on 10 parameters which were highlighted in the multivariate analysis, although further studies need to be addressed.

Conflicts of interest: None to declare.

Authors' contribution: V.R.P and A.C.F conceived the study. P.A.S., A.L. and T.V. designed the study. P.A.S. and A.L. interpreted the computed tomography scans. P.A.S. and D.V. applied the software. V.R.P., A.C.F., I.R., A.P. collected the data. V.R.P. drafted the paper. A.C.F. and A.H. revised the manuscript. N.A.H. supervised the study.

REFERENCES

1. Krumenacker JH, Panicek DM, Ginsberg MS, Bach AM, Hilton S, Schwartz LH. CT in searching for abscess after abdominal or pelvic surgery in patients with neoplasia: do abdomen and pelvis both need to be scanned? J Comput Assist Tomogr 1997;21:652-655. doi:10.1097/00004728-199707000-00026
2. Gnannt R, Fischer MA, Baechler T, et al. Distinguishing infected from noninfected abdominal fluid collections after surgery an imaging, clinical, and laboratory-based scoring system. Invest Radiol 2015;50:17-23. doi:10.1097/RLI.0000000000000090
3. Zimmerman LH, Tyburski JG, Glowniak J, et al. Impact of evaluating antibiotic concentrations in abdominal abscesses percutaneously drained. Am J Surg 2011;201:348-352. doi:10.1016/j.amjsurg.2010.09.010
4. Ariel IM, Kazarian KK. Classification, diagnosis and treatment of subphrenic abscesses. Rev Surg 1971;28:1-21.
5. Sirinek KR. Diagnosis and treatment of intra-abdominal abscesses. Surg Infect (Larchmt) 2000;1:31-38. doi:10.1089/109629600321272
6. Halber MD, Daffner RH, Morgan CL, et al. Intraabdominal abscess: current concepts in radiologic evaluation. AJR Am J Roentgenol 1979;133:9-13. doi:10.2214/ajr.133.1.9
7. Haaga JR, Alfidi RJ, Havrilla TR, et al. CT detection and aspiration of abdominal abscesses. AJR Am J Roentgenol 1977;128:465-474. doi:10.2214/ajr.128.3.465
8. Jaques P, Mauro M, Safrit H, Yankaskas B, Piggott B. CT features of intraabdominal abscesses: prediction of successful percutaneous drainage. AJR Am J Roentgenol1986;146:1041-1045. doi:10.2214/ajr.146.5.1041
9. Huang LL, Xia HH, Zhu SL. Ascitic Fluid Analysis in the Differential Diagnosis of Ascites: Focus on Cirrhotic Ascites. J Clin Transl Hepatol 2014;2:58-64. doi:10.14218/JCTH.2013.00010
10. Bala L, Sharma A, Yellapa RK, Roy R, Choudhuri G, Khetrapal CL. (1)H NMR spectroscopy of ascitic fluid: discrimination between malignant and benign ascites and comparison of the results with conventional methods. NMR Biomed 2008;21:606–614. doi:10.1002/nbm.1232
11. Csutak C, Ştefan PA, Lupean RA, Lenghel LM, Mihu CM, Lebovici A. Computed tomography in the diagnosis of intraperitoneal effusions: The role of texture analysis. Bosn J Basic Med Sci 2021;21:488-494. doi:10.17305/bjbms.2020.5048
12. Raveane W, Arrieta MAG. Texture Classification with Neural Networks. In: Omatu S, Neves J, Rodriguez JMC, Paz Santana JF, Gonzalez SR, editors. Distributed Computing and Artificial Intelligence, Cham: Springer International Publishing; 2013:325–328.
13. Varghese BA, Cen SY, Hwang DH, Duddalwar VA. Texture Analysis of Imaging: What Radiologists Need to Know. AJR Am J Roentgenol 2019;212:520–528. doi:10.2214/AJR.18.20624
14. Gillies RJ, Kinahan PE, Hricak H. Radiomics: images are more than pictures, they are data. Radiology 2016;278:563–577. doi:10.1148/radiol.2015151169
15. Li Z, Yu L, Wang X, et al. Diagnostic performance of mammographic texture analysis in the differential diagnosis of benign and malignant breast tumors. Clin Breast Cancer 2018;18:e621–e627. doi:10.1016/j.clbc.2017.11.004
16. Brynolfsson P, Nilsson D, Torheim T, et al. Haralick texture features from apparent diffusion coefficient (ADC) MRI images depend on imaging and pre-processing parameters. Sci Rep 2017;7:4041. doi:10.1038/s41598-017-04151-4
17. Matsuzaka M, Fukuda S, Takahashi I, et al. The decreasing burden of gastric cancer in Japan. Tohoku J Exp Med 2007;212:207–219. doi:10.1620/tjem.212.207
18. Meyer L, Meyer F, Dralle H, et al. Insufficiency risk of esophagojejunal anastomosis after total abdominal gastrectomy for gastric carcinoma. Langenbecks Arch Surg 2005;390:510–516. doi:10.1007/s00423-005-0575-2
19. Sauvanet A, Mariette C, Thomas P, et al. Mortality and morbidity after resection for adenocarcinoma of the gastroesophageal junction: predictive factors. J Am Coll Surg 2005;**201**:253–262. doi:10.1016/j.jamcollsurg.2005.02.002
20. Lang H, Piso P, Stukenborg C, Raab R, Jahne J. Management and results of proximal anastomotic leaks in a series of 1114 total gastrectomies for gastric carcinoma. Eur J Surg Oncol 2000;**26**:168–171. doi:10.1053/ejso.1999.0764
21. Wang P, Yang Z, He Y, Shu C. Pitfalls in the rapid diagnosis of positive blood culture. Rev Med Microbiol 2010;21:39–43. doi:10.1097/MRM.0b013e32833bb953
22. Kauss IAM, Grion CMC, Cardoso LTQ, et al. The epidemiology of sepsis in a Brazilian teaching hospital. Brazilian J Infect Dis 2010;14:264–270. doi:10.1016/S1413-8670(10)70054-4
23. Haaga JR, Alfidi RJ, Havrilla TR, et al. CT detection and aspiration of abdominal abscesses. AJR Am J Roentgenol 1977;128:465-474. doi:10.2214/ajr.128.3.465
24. Ferrucci JT Jr, vanSonnenberg E. Intra-abdominal abscess. Radiological diagnosis and treatment. JAMA 1981;246:2728-2733. doi:10.1001/jama.1981.03320230052028

25. Allen BC, Barnhart H, Bashir M, Nieman C, Breault S, Jaffe TA. Diagnostic accuracy of intra-abdominal fluid collection characterization in the era of multidetector computed tomography. Am Surg 2012;78:185-189.
26. Doi K. Computer-Aided Diagnosis in Medical Imaging: Historical Review, Current Status and Future Potential. Comput Med Imaging Graph 2007;31:198-211. doi:10.1016/j.compmedimag.2007.02.002
27. Tourassi GD. Journey toward computer-aided diagnosis: role of image texture analysis. Radiology 1999;213:317-320. doi:10.1148/radiology.213.2.r99nv49317
28. Castellano G, Bonilha L, Li LM, Cendes F. Texture analysis of medical images. Clin Radiol 2004;59:1061-1069. doi:10.1016/j.crad.2004.07.008
29. Raut A, Patil MA, Dhondrikar CP, Kamble SD. Texture Parameters Extraction of Satellite Image. IJSTE - Int J Sci Technol Eng 2016;2:2349-784X.
30. Csutak C, Stefan PA, Lenghel LM, et al. Differentiating High-Grade Gliomas from Brain Metastases at Magnetic Resonance: The Role of Texture Analysis of the Peritumoral Zone. *Brain Sci 2020;10:638. doi:*10.3390/brainsci10090638
31. Baroud, S, Schernthaner, R, Mayerhoefer, et al. Feasibility of Texture-based Classification of Different Types of Ascites at Contrast-enhanced Multidetector CT: Preliminary Results. Conference: Radiological Society of North America 2011 Scientific Assembly and Annual Meeting, November 26 - December 2, 2011, Chicago.